Articles in PresS. Am J Physiol Endocrinol Metab (July 18, 2017). doi:10.1152/ajpendo.00147.2017

Protein Kinase N2 Regulates AMP-Kinase Signaling and Insulin Responsiveness of Glucose Metabolism in Skeletal Muscle

Maxwell A. Ruby*, Isabelle Riedl*, Julie Massart*, Marcus Åhlin*, and Juleen R. Zierath*,‡

*Department of Molecular Medicine and Surgery, Section for Integrative Physiology, Karolinska Institutet, Stockholm, Sweden.

‡To whom correspondence should be addressed at: E-mail: Juleen.Zierath@ki.se

Author contributions: M.A.R., I.R., J.M. and M.Å. designed and performed research; M.A.R. and J.R.Z. designed research, analyzed data, and wrote the paper.

Running Title: Regulation of Skeletal Muscle Metabolism by PKN2

Keywords: Protein Kinase N2, Insulin Resistance, Skeletal Muscle, AMP Kinase, Lipid Metabolism

Copyright © 2017 by the American Physiological Society.

Abstract

Insulin resistance is central to the development of type 2 diabetes and related metabolic disorders. As skeletal muscle is responsible for the majority of whole body insulin-stimulated glucose uptake, regulation of glucose metabolism in this tissue is of particular importance. While Rho GTPases and many of their affecters influence skeletal muscle metabolism, there is a paucity of information on the protein kinase N (PKN) family of serine/threonine protein kinases. We investigated the impact of PKN2 on insulin signaling and glucose metabolism in primary human skeletal muscle cells *in vitro* and mouse tibialis anterior muscle *in vivo*. PKN2 knockdown *in vitro* decreased insulin-stimulated glucose uptake, incorporation into glycogen and oxidation. PKN2 siRNA increased 5' adenosine monophosphate-activated protein kinase (AMPK) signaling, while stimulating fatty acid oxidation and incorporation into triglycerides, and decreasing protein synthesis. At the transcriptional level, PKN2 knockdown increased expression of PGC1α and SREBP1c and their target genes. In mature skeletal muscle, *in vivo* PKN2 knockdown decreased glucose uptake and increased AMPK phosphorylation. Thus, PKN2 alters key signaling pathways and transcriptional networks to regulate glucose and lipid metabolism. Identification of PKN2 as a novel regulator of insulin and AMPK signaling may provide an avenue for manipulation of skeletal muscle metabolism.

Word count: 200/200

INTRODUCTION

As skeletal muscle is the predominant site of insulin-stimulated glucose uptake, skeletal muscle insulin resistance is a major contributing factor to defective blood glucose disposal in type 2 diabetes (5, 6). The physiological role of novel and previously identified candidate genes/proteins that regulate inter- and intra-cellular signaling pathways controlling cellular and whole body glucose and lipid homeostasis is an active area of current research. Through the discovery of key regulatory proteins in glucose and energy homeostasis, new diabetes prevention and treatment targets may be identified.

The Rho family of guanosine triphosphatases (GTPases), comprised of Rho, Rac and CDC42, are essential regulators of diverse biological functions including glucose metabolism. In particular, Rac1 is essential for both insulin-dependent and independent glucose uptake in skeletal muscle (31, 32). Rho GTPases utilize protein kinases to elicit many of their downstream effects. Among the Ser/Thr kinases that function as Rho GTPase effector molecules are Rho- (ROCK1/2), p21-activated (PAK1-PAK6), and protein kinase N (PKN1-PKN3) kinases (38). While members of the ROCK and PAK family have well-established roles in glucose metabolism and insulin signaling, little is known regarding the function of PKNs in skeletal muscle metabolic regulation (12, 33, 34).

PKNs are members of the atypical protein kinase C subfamily known for regulating actin cytoskeletal rearrangement and cell migration. While the three mammalian PKN family members share a large degree of homology in their C-terminal catalytic domain, variation in their regulatory domain results in selectivity to upstream signals (17, 21). Both PKN1 and PKN2 respond to Rho and Rac, but these isoforms display differential responsiveness to lipids and binding partner proteins (10, 11, 13, 21, 24, 26). Importantly, PKN2 represents the majority of Rho associated autophosphorylation activity in all tissues tested (36). A high

degree of isoform selectivity was confirmed by the finding that mice lacking PKN1, PKN3 or both are without overt phenotype, while loss of PKN2 is embryonically lethal (25).

In addition to Rho GTPases, phosphoinositide-dependent kinase-1 (PDK1), a key kinase in the insulin signaling cascade, stimulates PKNs by phosphorylation of the activation loop (9). In adipocytes, insulin stimulates PKN activity and PKN1 transmits the insulin signal to the actin cytoskeleton (9, 30). Conversely, PKNs may inhibit insulin signaling by directly interacting with PDK1 and Akt (8, 15, 35). In C2C12 cells, PKN2 contributes to cell adhesion-mediated activation of Akt (18). Moreover, phosphoproteomics of $PKN2^{-/-}$ mouse embryonic fibroblasts revealed elevations in the Akt pathway (25). As PKN2 is the predominant PKN isoform in skeletal muscle, we investigated a potential role for PKN2 in metabolic regulation in this tissue (7). We found that PKN2 knockdown impairs insulin responsive glucose metabolism and, unexpectedly, activates 5' adenosine monophosphate-activated protein kinase (AMPK) with downstream effects on lipid and protein metabolism.

MATERIALS AND METHODS

Cell culture and transfection.

Primary human skeletal muscle cell (HSMCs) cultures were established from *vastus lateralis* biopsies taken from healthy men as previously described (1). Cells were grown and differentiated as previously described (19). On days 4 and 6 of differentiation, myotubes were transfected with 25 nM small interfering RNA (siRNA) targeting PKN2 or scrambled control (781 and Negative Control No. 2, respectively, Ambion) utilizing Lipofectamine RNAiMax (Invitrogen) according to manufacturer's instructions. All experiments were performed on day 8 of differentiation. Hek293 cells were grown in DMEM (#31966, Thermofisher) supplemented with 10% FBS. Cells were co-transfected with siRNA (25 nM) and plasmid (1 μg/ml) utilizing Lipofectamine 2000 (Invitrogen) according to manufacturer's instructions 48 h prior to harvest. The plasmid encoding constitutively active Fyn kinase was a gift from Dr. Jeffrey Pessin (37). All experiments were performed in technical triplicate and results were normalized to protein content determined by the bicinchoninic acid assay (Pierce) with the exception of lipid fate. DNA content was quantified by the Qubit dsDNA HS assay (Thermofisher).

Glucose uptake, incorporation into glycogen and glucose oxidation in HSMCs

2-deoxyglucose uptake was measured as previously described (19). Briefly, 4 h serum starved HSMCs were incubated with 120 nM insulin or vehicle control for one hour. Following a PBS wash, glucose free media with ^{3}H 2-deoxyglucose and 10 μM 2-deoxyglucose was added to the cells for 15 minutes. Cells were lysed in 0.03% SDS and the lysate analysed for protein concentration and ^{3}H content. Glucose incorporation into glycogen was determined as previously described (22). Transfected HSMCs were incubated in the absence or presence of 120 nM insulin for 2 hours with an addition of ^{14}C-glucose for the final 90 minutes. Glycogen was precipitated from cell lysate and analyzed for ^{14}C content. Glucose oxidation

was performed as previously described (2). Transfected HSMCs were incubated with ^{14}C-glucose in the absence or presence of 120 nM insulin. Plates were sealed for 4 h to accumulate radioactive $^{14}CO_2$, which was captured and analyzed in 2 M NaOH following acidification of the media with 2 M HCl.

Fatty Acid Oxidation and lipid fate.

Fatty acid oxidation was measured as previously described (22). HSMCs were incubated in media with ^{3}H-palmitate and 25 μM of unlabeled palmitate with or without 5-aminoimidazole-4-carboxamide-1-β-4-ribofuranoside (AICAR) (2 mM). Following 6 hours incubation, palmitate was stripped from the media by incubation with charcoal and ^{3}H content in the palmitate-free media assessed. Lipid fate was measured as previously described (20). Transfected HSMCs were incubated with ^{14}C-palmitate in the absence or presence of AICAR (2 mM) for 6 hours. Total cellular lipids were extracted utilizing isopropanol-hexane-KCl (2:4:1), dried, reconstituted in chloroform/methanol (1:1), spotted on thin-layer chromatography (TLC) plates (Whatman), and separated in a hexane-diethylether-acetic acid (80:20:3) system. Lipid species were quantified by autoradiography.

Protein synthesis

Transfected HSMCs were incubated with ^{3}H-phenylalanine and 2 mM unlabeled phenylalanine for 6 hours. Following 4 washes with ice cold PBS, cells were lysed in 0.03% SDS. ^{3}H content was determined in trichloroacetic acid precipitate of the cell lysate.

Animals and in vivo experimental protocol.

All animal procedures have been approved by the Regional Animal Ethical Committee of Northern Stockholm. Male C57BL/6J mice (12–14 weeks old) were purchased from Charles

River (Sulzfeld, Germany) and acclimatized for at least 1 week before use. Mice were housed in a humidity- and temperature-controlled environment with 12h light:12h darkness cycle and provided *ad libitum* access to water and standard rodent chow (4% fat, 16.5% protein, 58% carbohydrates, 3.0kcal/g purchased from Lantmännen, Stockholm, Sweden). *Tibialis anterior* muscles of adult C57BL/6J mice were transfected with either Sure Silencing GFP negative control or a mixture of 4 plasmids encoding short hairpin RNAs (shRNAs) targeting PKN2 (KM34588G, Qiagen) by electroporation as described previously (16). One week after electroporation, mice were fasted for 4h and subjected to a modified oral glucose tolerance test to assess glucose uptake into skeletal muscle, as described (16). Glycogen content was determined as previously described (19). For insulin signaling experiments, male C57BL/6J mice (12 weeks old) were fasted for 4 h and treated I.P. with insulin (5 units/kg) or saline for 15 min. Mice were anesthetized with Avertin and electroporated or quadriceps muscle removed and frozen immediately.

Western Blot analysis.

Transfected cells were harvested, placed on Laemmli buffer and subjected to Western Blot analysis as previously described (19). Ponceau staining was used to confirm equal protein loading. Membranes were also probed against β-actin to control for equal loading of proteins. Proteins were quantified by densitometry utilizing Quantity One Software (Bio-Rad). The quantifications displaying statistical significance or trends ($p<0.1$) are presented in the manuscript in graphical format. Antibodies used are given in Table 1.

RNA extraction and mRNA expression quantification.

mRNA was extracted from HSMC and skeletal muscle tissue with the RNeasy Mini Kit (Qiagen,) and TRIzol reagent (Invitrogen,) respectively, according to the manufacturer's

recommendations. cDNA synthesis and semi-quantitative real-time PCR was performed as previously described (19). Primer sequences are presented in Table 2.

Statistical analysis.

Statistical analyses were performed using GraphPad Prism 7.0 (GraphPad Software. San Diego, CA). Two-way analysis of variance was performed on untransformed data to assess the effects of siRNA and compounds. Data is presented as fold change to remove inter-cell line variation for visualization purposes. Paired *t*-test analysis was utilized for single variable experiments. Significance was set at $p<0.05$. Data is presented as mean ± SEM.

RESULTS

Gene silencing of PKN2 does not alter myotube differentiation.

To assess the impact of PKN2 on skeletal muscle metabolism, primary human skeletal muscle cells were transfected with PKN2 siRNA on days 4 and 6 after the initiation of differentiation. This treatment achieved a robust knockdown of PKN2 mRNA and protein (Fig 1A and 1B). As PKN2 regulates myotube differentiation in C2C12 cells (18), we sought to ensure that PKN2 knockdown did not alter the differentiation status of the human myotubes used here. Visual appearance of cultures, as well as mRNA expression and protein abundance of myogenic (desmin) and proliferative markers (PAX7) were unchanged (Fig 1A, 1B and 1C). Myotube protein to DNA ratio was unchanged by siRNA treatment (Scr: 0.84±0.07 mg protein/mg DNA; PKN2: 0.86±0.05 mg protein/mg DNA; n=5).

Role of PKN2 in glucose metabolism and insulin signaling.

Having established that PKN2 knockdown does not alter the differentiation status of HSMCs, we utilized radioactive tracer based methods to assess glucose metabolism. PKN2 knockdown decreased insulin-stimulated glucose uptake and incorporation into glycogen without altering basal glucose metabolism (Fig 1D and 1E). Similarly, insulin-stimulated glucose oxidation was diminished in cells depleted of PKN2 (Fig 1F).

PKN2 has been reported to be phosphorylated by PDK1 (9). Given that PKN2 knockdown diminished insulin-responsiveness of glucose metabolism, we sought to determine if PKN2 constitutes a branch of, or otherwise influences, insulin signaling. Western blot analysis revealed that insulin treatment of either HSMC (Fig 2A) or mouse quadriceps muscle (Fig 2B) did not alter phosphorylation of the activation loop in either PKN2 or PKN1. PKN2 knockdown did not alter the phosphorylation of Akt or GSK3α/β (Fig 2A). However, PKN2 knockdown increased phosphorylation of TBC1D4 under both basal

and insulin-stimulated conditions in HSMC (Fig 2A, 2C). Thus, the activation loop of PKN2 does not appear to be phosphorylated in response to insulin. Furthermore, decreased insulin-stimulated glucose metabolism in PKN2 knockdown cells cannot be explained by altered phosphorylation within the canonical insulin signaling cascade.

PKN2 gene silencing increases AMPK signaling.

As PKN2 knockdown impaired insulin-responsiveness of glucose metabolism, we sought to examine whether PKN2 influences AMPK signaling. PKN2 knockdown increased the phosphorylation of AMPK and its substrate ACC (Fig 3A-C). Fyn kinase inhibits AMPK activity by sequestering LKB1 in the nucleus (37). As PKN2 activates Fyn kinase, we determined whether PKN2 knockdown increases AMPK signaling by decreasing Fyn kinase activity using constitutively active Fyn kinase (caFyn) in HEK293 cells (28, 37). Increased phosphorylation of ACC upon knockdown of PKN2 persisted, irrespective of caFyn overexpression (Fig 3D). Thus, PKN2 knockdown increases AMPK signaling independently of Fyn kinase.

PKN2 gene silencing increases lipid metabolism and genes involved in lipid handling.

To determine if PKN2 knockdown influences lipid metabolism, fatty acid oxidation and lipid fate was assessed in HSMC incubated in the absence or presence of the AMPK activator AICAR. PKN2 knockdown increased both basal and AICAR-stimulated fatty acid oxidation (Fig 4A). Similar to AICAR treatment, PKN2 knockdown decreased palmitate incorporation into 1,3-diacylglycerol and the origin, which contains polar lipids (Fig 4B). Interestingly, PKN2 markedly increased incorporation of palmitate into triglycerides (Fig 4B). To gain insight into mechanisms by which PKN2 alters lipid metabolism, we performed qPCR analysis of genes involved in lipid handling and synthesis. PKN2 knockdown increased

expression of the transcriptional co-activator PGC-1α and several of its target genes (CPT1β, PDK4, FABP3) (Fig 4C). PKN2 silencing also increased expression of genes involved in fatty acid synthesis (SCD1, FASN, SREBP1c) and, unexpectedly, decreased the expression of genes involved in triglyceride synthesis (DGAT1 and GPAT1) (Fig 4D).

PKN2 gene silencing decreased mTOR signaling and protein synthesis.

As PKN2 knockdown led to increased AMPK signaling, we determined whether downstream targets involved in protein metabolism might also be altered. Consistent with AMPK activation, PKN2 knockdown decreased both basal and insulin-stimulated phosphorylation of mTOR and S6 ribosomal protein (Fig 5A-C). To determine whether these changes were associated with alterations in protein metabolism, we performed a protein synthesis assay. PKN2 knockdown decreased incorporation of phenylalanine into protein (Fig 5D). Consistent with AMPK activation, PKN2 knockdown decreased mTOR signaling and protein synthesis.

PKN2 knockdown in mature skeletal muscle.

To assess the impact of PKN2 gene silencing in mature skeletal muscle *in vivo*, contralateral tibialis anterior muscles were electroporated with shRNA targeting PKN2 or a scrambled control sequence. PKN2 shRNA produced a modest decrease in both PKN2 mRNA expression (77±11% of control leg) and protein abundance (Fig 6A, 6B). To determine whether PKN2 gene silencing affects glucose uptake in adult skeletal muscle *in vivo*, we performed a modified oral glucose tolerance test utilizing radiolabeled 2-deoxyglucose. PKN2 depletion reduced glucose uptake in tibialis anterior muscle (Fig 6C). Similarly, PKN2 silencing was associated with a trend ($p=0.07$) for decreased glycogen content in skeletal muscle (Fig 6D). We next determined whether PKN2 silencing activates AMPK signaling, by assessing phosphorylation of AMPK and its substrate ACC in adult skeletal muscle. Similar

to our *in vitro* results, PKN2 silencing was associated with an increase in the phosphorylation of AMPK (Fig 6A, 6E) and its substrate ACC, although ACC phosphorylation did not reach statistical significance (Fig 6A, 6F). Thus, PKN2 knockdown *in vivo* inhibits glucose uptake during a glucose challenge and activates AMPK signaling in mature skeletal muscle.

DISCUSSION

Insulin and AMPK are powerful regulators of metabolism in skeletal muscle. Insulin favors cell growth and energy storage, while AMPK signals energy stress within the cell to favor catabolic processes. Here, we provide evidence that PKN2 depletion in skeletal muscle impairs insulin-responsiveness of glucose metabolism and augments AMPK signaling with concomitant effects on protein and lipid metabolism. The late initiation and duration of PKN2 knockdown utilized in the present study may explain the non-effects on myotube differentiation and hypotrophy, despite previous findings in C2C12 cells and observed decreases in protein synthesis, respectively (18).

A complex network of insulin-regulated signals control glucose metabolism. These signals include Rho GTPases and their effector molecules. As PKN2 silencing reduced insulin-simulated glucose uptake in HSMCs and glucose uptake during a glucose challenge in adult skeletal muscle, it may function as an effector protein in the insulin signaling network. Given that PKN2 knockdown impairs insulin-stimulated glucose uptake despite stimulating two distinct signals, phosphorylation of TBC1D4 on Ser^{318} and activation of AMPK, that normally stimulate glucose uptake, PKN2 likely functions downstream of Rab GTPases to facilitate insulin-stimulated glucose metabolism. PKN2 is known to regulate the cytoskeleton (36). Thus, PKN2 may play a role in relaying the insulin signal to the cytoskeleton in skeletal muscle by a mechanism analogous to that of PKN1 in adipocytes (9). The exact nature of PKN2's role in transducing the insulin signal to downstream targets remains unclear. Although we could not detect alterations in PKN2 phosphorylation in response to insulin, we cannot exclude the possibility that insulin treatment alters PKN2 activity or localization (30).

Aside from a potential role within the insulin signaling cascade, PKN2 has been shown to influence Akt signaling both by directly binding to PDK1 and indirectly influencing its activity (8, 15, 35). Unbiased phosphoproteomic studies reveal Akt signaling is decreased in

PKN2$^{-/-}$ mouse embryonic fibroblasts (25). While we did not detect changes in Akt or GSK3α/β phosphorylation, we found phosphorylation of Ser^{318} on TBC1D4 was increased upon PKN2 knockdown. Serine 318 on TBC1D4 is phosphorylated by Akt in response to insulin, but not by AMPK activation. Target and context specific activation of Akt signaling is supported by the finding that PKN2 functions in a complex with adaptor protein, phosphotyrosine interacting with PH domain and leucine zipper 1 (APPL1) and cell adhesion molecule-related downregulated by oncogene (CDO) to increase Akt phosphorylation in differentiating, but not proliferating, myoblasts (18). Interestingly, APPL1 inhibition phenocopies the effect of PKN2 silencing on glucose uptake, glycogen content and AMPK signaling (4). Thus, APPL1 and PKN2 may share common points of action in the regulation of glucose metabolism. Another member of the APPL family, APPL2, has been shown to interact with TBC1D1 and control its phosphorylation (3). The mechanism by which PKN2 influences TBC1D4 phosphorylation requires further study.

AMPK is a cellular energy sensor that influences lipid, glucose, and protein metabolism, as well as gene expression. PKN2 depletion *in vitro* and *in vivo* augments AMPK signaling, but the mechanism is unclear. PKN2 activates Fyn kinase to regulate cell adhesion in keratinocytes (28). Notably, Fyn kinase-induced phosphorylation of LKB1 regulates AMPK activity by sequestering LKB1 in the nucleus (37). Thus, inhibition of Fyn kinase may be responsible for AMPK activation upon PKN2 knockdown. However, our finding of a persistent AMPK activation by PKN2 knockdown in the presence of constitutively active Fyn kinase demonstrates that Fyn kinase is dispensable. Interestingly, several Rho kinase inhibitors known to activate AMPK and influence obesity-related insulin resistance also inhibit PKN2 (14, 23).

AMPK signaling inhibits mTOR and ACC to decrease protein synthesis and increase lipid oxidation, respectively. Consistent with activation of AMPK, PKN2 knockdown decreased

protein synthesis and stimulated fatty acid oxidation. Our findings that PKN2 knockdown decreased phosphorylation of mTOR and S6 ribosomal protein are consistent with decreased S6 kinase phosphorylation in PKN2$^{-/-}$ mouse embryonic fibroblasts (25). AMPK controls lipid metabolism by phosphorylating ACC, as well as by activating transcriptional regulators. PKN2 knockdown increased expression of PGC1α and several of its target genes (29). Despite decreased expression of genes involved in triglyceride synthesis, PKN2 knockdown increased palmitate incorporation into triglycerides. This altered partitioning of fatty acids towards oxidation and triglyceride synthesis and away from diacylglycerol also occurs upon AMPK activation and in response to exercise (27).

Taken together our results demonstrate that PKN2 is a novel regulator of insulin-stimulated glucose metabolism and AMPK signaling in skeletal muscle. Additionally, our findings suggest that PKN2 knockdown phenocopies APPL1 inhibition, supporting the notion that these two proteins may function together in a signaling complex (4). Further understanding of the role of PKN2 in controlling key signaling and metabolic events in skeletal muscle could aid in the treatment of insulin resistance in type 2 diabetes.

Acknowledgements

The authors would like to thank Arja Kants for administrative help and Dr. Jeffrey Pessin for the Fyn constitutively active construct.

References

1. **Al-Khalili L, Bouzakri K, Glund S, Lonnqvist F, Koistinen HA, and Krook A**. Signaling specificity of interleukin-6 action on glucose and lipid metabolism in skeletal muscle. *Molecular endocrinology* 20: 3364-3375, 2006.
2. **Bouzakri K, Austin R, Rune A, Lassman ME, Garcia-Roves PM, Berger JP, Krook A, Chibalin AV, Zhang BB, and Zierath JR**. Malonyl CoenzymeA decarboxylase regulates lipid and glucose metabolism in human skeletal muscle. *Diabetes* 57: 1508-1516, 2008.
3. **Cheng KK, Zhu W, Chen B, Wang Y, Wu D, Sweeney G, Wang B, Lam KS, and Xu A**. The adaptor protein APPL2 inhibits insulin-stimulated glucose uptake by interacting with TBC1D1 in skeletal muscle. *Diabetes* 63: 3748-3758, 2014.
4. **Cleasby ME, Lau Q, Polkinghorne E, Patel SA, Leslie SJ, Turner N, Cooney GJ, Xu A, and Kraegen EW**. The adaptor protein APPL1 increases glycogen accumulation in rat skeletal muscle through activation of the PI3-kinase signalling pathway. *J Endocrinol* 210: 81-92, 2011.
5. **DeFronzo RA, Gunnarsson R, Bjorkman O, Olsson M, and Wahren J**. Effects of insulin on peripheral and splanchnic glucose metabolism in noninsulin-dependent (type II) diabetes mellitus. *The Journal of clinical investigation* 76: 149-155, 1985.
6. **DeFronzo RA, Jacot E, Jequier E, Maeder E, Wahren J, and Felber JP**. The effect of insulin on the disposal of intravenous glucose. Results from indirect calorimetry and hepatic and femoral venous catheterization. *Diabetes* 30: 1000-1007, 1981.
7. **Deshmukh AS, Murgia M, Nagaraj N, Treebak JT, Cox J, and Mann M**. Deep proteomics of mouse skeletal muscle enables quantitation of protein isoforms, metabolic pathways, and transcription factors. *Molecular & cellular proteomics : MCP* 14: 841-853, 2015.
8. **Dettori R, Sonzogni S, Meyer L, Lopez-Garcia LA, Morrice NA, Zeuzem S, Engel M, Piiper A, Neimanis S, Frodin M, and Biondi RM**. Regulation of the interaction between protein kinase C-related protein kinase 2 (PRK2) and its upstream kinase, 3-phosphoinositide-dependent protein kinase 1 (PDK1). *The Journal of biological chemistry* 284: 30318-30327, 2009.
9. **Dong LQ, Landa LR, Wick MJ, Zhu L, Mukai H, Ono Y, and Liu F**. Phosphorylation of protein kinase N by phosphoinositide-dependent protein kinase-1 mediates insulin signals to the actin cytoskeleton. *Proceedings of the National Academy of Sciences of the United States of America* 97: 5089-5094, 2000.
10. **Flynn P, Mellor H, Casamassima A, and Parker PJ**. Rho GTPase control of protein kinase C-related protein kinase activation by 3-phosphoinositide-dependent protein kinase. *The Journal of biological chemistry* 275: 11064-11070, 2000.
11. **Flynn P, Mellor H, Palmer R, Panayotou G, and Parker PJ**. Multiple interactions of PRK1 with RhoA. Functional assignment of the Hr1 repeat motif. *The Journal of biological chemistry* 273: 2698-2705, 1998.
12. **Furukawa N, Ongusaha P, Jahng WJ, Araki K, Choi CS, Kim HJ, Lee YH, Kaibuchi K, Kahn BB, Masuzaki H, Kim JK, Lee SW, and Kim YB**. Role of Rho-kinase in regulation of insulin action and glucose homeostasis. *Cell metabolism* 2: 119-129, 2005.
13. **Gross C, Heumann R, and Erdmann KS**. The protein kinase C-related kinase PRK2 interacts with the protein tyrosine phosphatase PTP-BL via a novel PDZ domain binding motif. *FEBS letters* 496: 101-104, 2001.
14. **Kanda T, Wakino S, Homma K, Yoshioka K, Tatematsu S, Hasegawa K, Takamatsu I, Sugano N, Hayashi K, and Saruta T**. Rho-kinase as a molecular target for

insulin resistance and hypertension. *FASEB journal : official publication of the Federation of American Societies for Experimental Biology* 20: 169-171, 2006.
15. **Koh H, Lee KH, Kim D, Kim S, Kim JW, and Chung J**. Inhibition of Akt and its anti-apoptotic activities by tumor necrosis factor-induced protein kinase C-related kinase 2 (PRK2) cleavage. *J Biol Chem* 275: 34451-34458, 2000.
16. **Kulkarni SS, Karlsson HK, Szekeres F, Chibalin AV, Krook A, and Zierath JR**. Suppression of 5'-nucleotidase enzymes promotes AMP-activated protein kinase (AMPK) phosphorylation and metabolism in human and mouse skeletal muscle. *The Journal of biological chemistry* 286: 34567-34574, 2011.
17. **Lachmann S, Jevons A, De Rycker M, Casamassima A, Radtke S, Collazos A, and Parker PJ**. Regulatory domain selectivity in the cell-type specific PKN-dependence of cell migration. *PloS one* 6: e21732, 2011.
18. **Lee SJ, Hwang J, Jeong HJ, Yoo M, Go GY, Lee JR, Leem YE, Park JW, Seo DW, Kim YK, Hahn MJ, Han JW, Kang JS, and Bae GU**. PKN2 and Cdo interact to activate AKT and promote myoblast differentiation. *Cell Death Dis* 7: e2431, 2016.
19. **Massart J, Sjogren RJ, Lundell LS, Mudry JM, Franck N, O'Gorman DJ, Egan B, Zierath JR, and Krook A**. Altered miRNA-29 Expression in Type 2 Diabetes Influences Glucose and Lipid Metabolism in Skeletal Muscle. *Diabetes* 2017.
20. **Massart J, Zierath JR, and Chibalin AV**. A simple and rapid method to characterize lipid fate in skeletal muscle. *BMC research notes* 7: 391, 2014.
21. **Mukai H**. The structure and function of PKN, a protein kinase having a catalytic domain homologous to that of PKC. *Journal of biochemistry* 133: 17-27, 2003.
22. **Nascimento EB, Riedl I, Jiang LQ, Kulkarni SS, Naslund E, and Krook A**. Enhanced glucose metabolism in cultured human skeletal muscle after Roux-en-Y gastric bypass surgery. *Surg Obes Relat Dis* 11: 592-601, 2015.
23. **Noda K, Nakajima S, Godo S, Saito H, Ikeda S, Shimizu T, Enkhjargal B, Fukumoto Y, Tsukita S, Yamada T, Katagiri H, and Shimokawa H**. Rho-kinase inhibition ameliorates metabolic disorders through activation of AMPK pathway in mice. *PLoS One* 9: e110446, 2014.
24. **Owen D, Lowe PN, Nietlispach D, Brosnan CE, Chirgadze DY, Parker PJ, Blundell TL, and Mott HR**. Molecular dissection of the interaction between the small G proteins Rac1 and RhoA and protein kinase C-related kinase 1 (PRK1). *The Journal of biological chemistry* 278: 50578-50587, 2003.
25. **Quetier I, Marshall JJ, Spencer-Dene B, Lachmann S, Casamassima A, Franco C, Escuin S, Worrall JT, Baskaran P, Rajeeve V, Howell M, Copp AJ, Stamp G, Rosewell I, Cutillas P, Gerhardt H, Parker PJ, and Cameron AJ**. Knockout of the PKN Family of Rho Effector Kinases Reveals a Non-redundant Role for PKN2 in Developmental Mesoderm Expansion. *Cell reports* 14: 440-448, 2016.
26. **Quilliam LA, Lambert QT, Mickelson-Young LA, Westwick JK, Sparks AB, Kay BK, Jenkins NA, Gilbert DJ, Copeland NG, and Der CJ**. Isolation of a NCK-associated kinase, PRK2, an SH3-binding protein and potential effector of Rho protein signaling. *The Journal of biological chemistry* 271: 28772-28776, 1996.
27. **Schenk S, and Horowitz JF**. Acute exercise increases triglyceride synthesis in skeletal muscle and prevents fatty acid-induced insulin resistance. *J Clin Invest* 117: 1690-1698, 2007.
28. **Schmidt A, Durgan J, Magalhaes A, and Hall A**. Rho GTPases regulate PRK2/PKN2 to control entry into mitosis and exit from cytokinesis. *The EMBO journal* 26: 1624-1636, 2007.
29. **Srivastava RA, Pinkosky SL, Filippov S, Hanselman JC, Cramer CT, and Newton RS**. AMP-activated protein kinase: an emerging drug target to regulate imbalances

in lipid and carbohydrate metabolism to treat cardio-metabolic diseases. *Journal of lipid research* 53: 2490-2514, 2012.
30. **Standaert M, Bandyopadhyay G, Galloway L, Ono Y, Mukai H, and Farese R**. Comparative effects of GTPgammaS and insulin on the activation of Rho, phosphatidylinositol 3-kinase, and protein kinase N in rat adipocytes. Relationship to glucose transport. *The Journal of biological chemistry* 273: 7470-7477, 1998.
31. **Sylow L, Jensen TE, Kleinert M, Hojlund K, Kiens B, Wojtaszewski J, Prats C, Schjerling P, and Richter EA**. Rac1 signaling is required for insulin-stimulated glucose uptake and is dysregulated in insulin-resistant murine and human skeletal muscle. *Diabetes* 62: 1865-1875, 2013.
32. **Sylow L, Jensen TE, Kleinert M, Mouatt JR, Maarbjerg SJ, Jeppesen J, Prats C, Chiu TT, Boguslavsky S, Klip A, Schjerling P, and Richter EA**. Rac1 is a novel regulator of contraction-stimulated glucose uptake in skeletal muscle. *Diabetes* 62: 1139-1151, 2013.
33. **Tunduguru R, Chiu TT, Ramalingam L, Elmendorf JS, Klip A, and Thurmond DC**. Signaling of the p21-activated kinase (PAK1) coordinates insulin-stimulated actin remodeling and glucose uptake in skeletal muscle cells. *Biochemical pharmacology* 92: 380-388, 2014.
34. **Wang Z, Oh E, Clapp DW, Chernoff J, and Thurmond DC**. Inhibition or ablation of p21-activated kinase (PAK1) disrupts glucose homeostatic mechanisms in vivo. *The Journal of biological chemistry* 286: 41359-41367, 2011.
35. **Wick MJ, Dong LQ, Riojas RA, Ramos FJ, and Liu F**. Mechanism of phosphorylation of protein kinase B/Akt by a constitutively active 3-phosphoinositide-dependent protein kinase-1. *J Biol Chem* 275: 40400-40406, 2000.
36. **Vincent S, and Settleman J**. The PRK2 kinase is a potential effector target of both Rho and Rac GTPases and regulates actin cytoskeletal organization. *Molecular and cellular biology* 17: 2247-2256, 1997.
37. **Yamada E, Pessin JE, Kurland IJ, Schwartz GJ, and Bastie CC**. Fyn-dependent regulation of energy expenditure and body weight is mediated by tyrosine phosphorylation of LKB1. *Cell metabolism* 11: 113-124, 2010.
38. **Zhao ZS, and Manser E**. PAK and other Rho-associated kinases--effectors with surprisingly diverse mechanisms of regulation. *The Biochemical journal* 386: 201-214, 2005.

456 **Table 1: Antibodies Used**

Target	Catalogue #	Company
PKN2 (cells)	8697	Cell Signaling
PAX7	27-583	Prosci, Inc
DES	15200	Abcam
β-ACTIN	A5541	Sigma
Phospho-PKN1/2 ($Thr^{774/816}$)	2611	Cell Signaling
Phospho-Akt (Ser^{473})	9271	Cell Signaling
Phospho-Akt (Thr^{308})	4056	Cell Signaling
Akt	9272	Cell Signaling
Phospho-GSK-3α/β ($Ser^{21/9}$)	9331	Cell Signaling
GSK3 β	9315	Cell Signaling
P-TBC1D4	8619	Cell Signaling
TBC1D4	07-741	EMB Millipore
Phospho-mTOR (Ser^{2448})	5536	Cell Signaling
mTOR (7C10)	2983	Cell Signaling
P-AMPK (Thr^{172})	2531	Cell Signaling
AMPK	2532	Cell Signaling
P-ACC (Ser^{79})	3661	Cell Signaling
ACC	3676	Cell Signaling
Fyn	sc-16	Santa Cruz
GAPDH	25778	Santa Cruz
P-S6 ($Ser^{235/236}$)	2211	Cell Signaling
S6	2317	Cell Signaling
PKN2 (mouse muscle)	2612	Cell Signaling

457

458

459

460 **Table 2: Primers Used**

Human	**Forward**	**Reverse**
rplo	TGGAGAAACTGCTGCCTCAT	GATTTCAATGGTGCCCCTGG
ppia	AGGGTTCCTGCTTTCACAGA	CAGGACCCGTATGCTTTAGG
pkn2	ATTGTGGCTCGAGATGAAGT	TTTGGTTTGGAAACATGCAA
pax7	GAGGACCAAGCTGACAGAGG	CTGGCAGAAGGTGGTTGAA
myog	GCTCAGCTCCCTCAACCA	GCTGTGAGAGCTGCATTCG
des	CTGGAGCGCAGAATTGAATC	GGCAGTGAGGTCTGGCTTAG
ppara	TTCGCAATCCATCGGCGAG	CCACAGGATAAGTCACCGAGG
ppard	CAGGGCTGACTGCAAACGA	CTGCCACAATGTCTCGATGTC
pgc1a	TCTGAGTCTGTATGGAGTGACAT	CCAAGTCGTTCACATCTAGTTCA
cpt1b	CATGTATCGCCGTAAACTGGAC	TGGTAGGAGCACATAGGCACT
fabp3	TGGAGTTCGATGAGACAACAGC	CTCTTGCCCGTCCCATTTCTG
pdk4	GGAAGCATTGATCCTAACTGTGA	GGTGAGAAGGAACATACACGATG
srebp1c	GTTGGCCCTACCCCTCC	CTTCAGCGAGGCGGCTT
fasn	CCACAACTCCAAGGACACAG	CTGCTCCACGAACTCAAACA
scd1	CCTGCGGATCTTCCTTATCA	GCCCATTCGTACACGTCATT
acc2	CTGAGAGTGCGGAGGACTTC	AGCGAGGATCTGAACTTCCA
dgat1	GTCCCTCTGCGAATGTTCC	GCTATTGGCTGTCCGATGAT
gpat1	AACACCAGATGGACGGAAAG	CCGAGCACAAGAGGTTTTTC
Mouse	**Forward**	**Reverse**
pkn2	CGACCAAAACTCCAAAGACA	GTCTTCCCCAAGTGGCAATA
36b4	CCCTGAAGTGCTCGACATCA	TGCGGACACCCTCCAGAA

461

462

Figure Legends

Fig. 1. PKN2 knockdown decreases insulin responsiveness of glucose metabolism in skeletal muscle. (A) mRNA levels of PKN2, PAX7, MYOG (myogenin), and DES (desmin) and (B) protein abundance of PKN2, PAX7, and desmin in siRNA-treated primary HSMCs. (C) Representative brightfield images of siRNA-treated primary HSMC. Scale bar=100 µm. Basal and insulin-stimulated (120 nM) (D) glucose uptake, (E) incorporation into glycogen and (F) oxidation in siRNA-treated primary HSMC. Open bars: SCR, Closed Bars: siPKN2. *PKN2 effect, $p<0.05$. $^{\#}$Insulin main effect, $p<0.05$. Results are mean ± SEM for n=5 biological replicates.

Fig. 2. PKN2 knockdown increases TBC1D4 phosphorylation in HSMCs. (A) Western blot analysis of PKN2, Akt, GSK3, and TBC1D4 protein and phosphorylation from basal and insulin-stimulated (120 nM; 15 min) primary HSMCs (representative immunoblot from n=5 biological replicates). (B) Western blot analysis of PKN2 and Akt protein and phosphorylation in mouse quadriceps muscle 15 min following saline or insulin (5 IU/kg I.P.) injection (representative immunoblot from n=4 mice). (C) Quantification of P-TBC1D4^{Ser318} abundance in basal and insulin-stimulated primary HSMCs. Open bars: SCR, Closed Bars: siPKN2. *PKN2 effect, $p<0.05$. $^{\#}$Insulin main effect, $p<0.05$. Results are mean ± SEM for n=5 biological replicates.

Fig. 3. PKN2 knockdown increases AMPK signaling. (A) Western blot analysis of P-AMPK^{Thr172}, AMPK, and P-ACC^{Ser79} in primary HSMCs incubated in the absence or presence of insulin (120 nM; 15 min) (representative immunoblot from n=5 biological replicates). Quantification of (B) P-AMPK^{Thr172} and (C) P-ACC^{Ser79} abundance. (D) Western blot analysis of P-ACC^{Ser79} abundance in PKN2 siRNA-treated HEK293 cells overexpressing

caFYN (representative immunoblot from n=3 biological replicates). Open bars: SCR, Closed Bars: siPKN2. *PKN2 post-hoc effect. Results are mean ± SEM for n=5 biological replicates.

Fig. 4. **PKN2 knockdown increases fatty acid oxidation and incorporation into triglycerides.** Palmitate (A) oxidation and (B) incorporation into lipid species in siRNA treated primary HSMC incubated in the absence or presence of AICAR (2 mM). mRNA level of (C) PGC-1α and (D) SREBP1c target genes in siRNA-treated primary HSMCs. Open bars: SCR, Closed Bars: siPKN2. *PKN2 post-hoc effect, $p<0.05$. $^{\#}$AICAR main effect, $p<0.05$. Results are mean ± SEM for n=5 biological replicates.

Fig. 5. PKN2 knockdown decreases mTOR signaling and protein synthesis. (A) Western blot analysis P-mTOR^{Ser2448}, mTOR, P-S6$^{Ser235/236}$, and S6 in primary HSMCs incubated in the absence or presence of insulin (120 nM; 15 min) (representative immunoblot from n=5 biological replicates). Quantification of (B) P-mTOR^{Ser2448} and (C) P-S6$^{Ser235/236}$ abundance. (D) Protein synthesis in siRNA-treated primary HSMCs. *PKN2 effect, $p<0.05$. Open bars: SCR, Closed Bars: siPKN2. $^{\#}$Insulin main effect, $p<0.05$. Results are mean ± SEM for n=5 biological replicates.

Fig. 6. PKN2 silencing *in vivo* decreases glucose uptake and activates AMPK. Contralateral tibialis anterior muscles were electroporated with shRNA targeting PKN2 or scrambled control. Seven days following electroportation 4 h fasted mice were administered an oral glucose load (3 g/kg) followed by I.P. injection of ^{3}H-deoxyglucose. Tibialis anterior muscle was harvested 2 h following the oral glucose challenge and analyzed for: (A) PKN2, P-AMPK^{Thr172}, AMPK, P-ACC^{Ser79} and ACC protein abundance (representative immunoblot from n=7 mice). (B) Quantification of PKN2 protein abundance, (C) *in vivo* glucose uptake

(D) intramuscular glycogen content, (E) Quantification of P-AMPK^{Thr172} abundance and (F) P-ACC^{Ser79} abundance in PKN2 shRNA-treated mouse tibialis anterior muscle. *paired t-test, $p<0.05$. Results are mean ± SEM for n=7 mice.

Figure 1

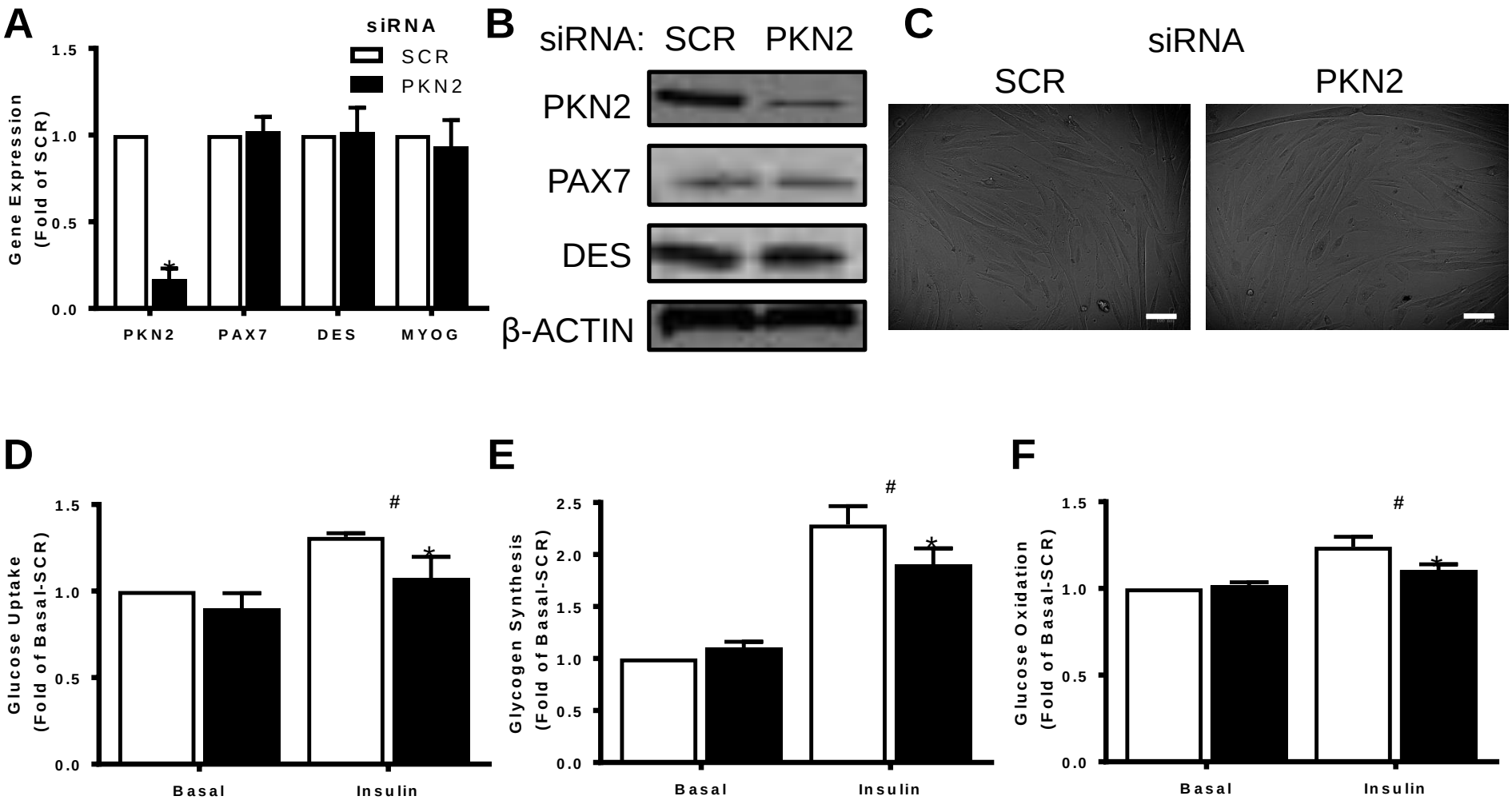
A
siRNA
SCR
PKN2
Gene Expression (Fold of SCR)
1.5
1.0
0.5
0.0
*
PKN2
PAX7
DES
MYOG
B
siRNA: SCR PKN2
PKN2
PAX7
DES
β-ACTIN
C
siRNA
SCR
PKN2
D
Glucose Uptake (Fold of Basal-SCR)
1.5
1.0
0.5
0.0
#
*
Basal
Insulin
E
Glycogen Synthesis (Fold of Basal-SCR)
2.5
2.0
1.5
1.0
0.5
0.0
#
*
Basal
Insulin
F
Glucose Oxidation (Fold of Basal-SCR)
1.5
1.0
0.5
0.0
#
*
Basal
Insulin

Figure 2

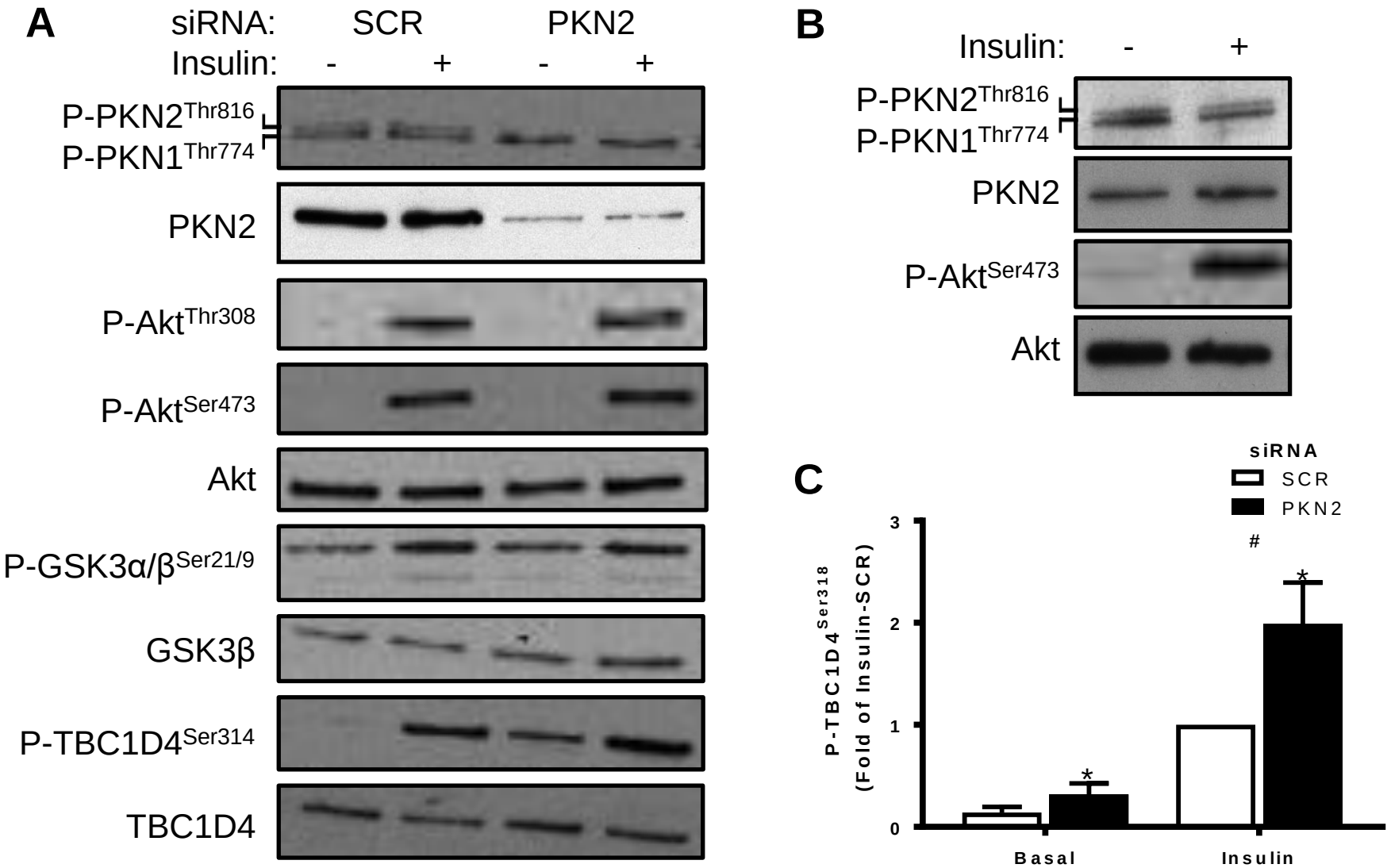
A
siRNA: SCR PKN2
Insulin: - + - +
P-PKN2Thr816
P-PKN1Thr774
PKN2
P-AktThr308
P-AktSer473
Akt
P-GSK3α/βSer21/9
GSK3β
P-TBC1D4Ser314
TBC1D4
B
Insulin: - +
P-PKN2Thr816
P-PKN1Thr774
PKN2
P-AktSer473
Akt
C
siRNA
SCR
PKN2
#
P-TBC1D4Ser318
(Fold of Insulin-SCR)
3
2
1
0
*
*
Basal
Insulin

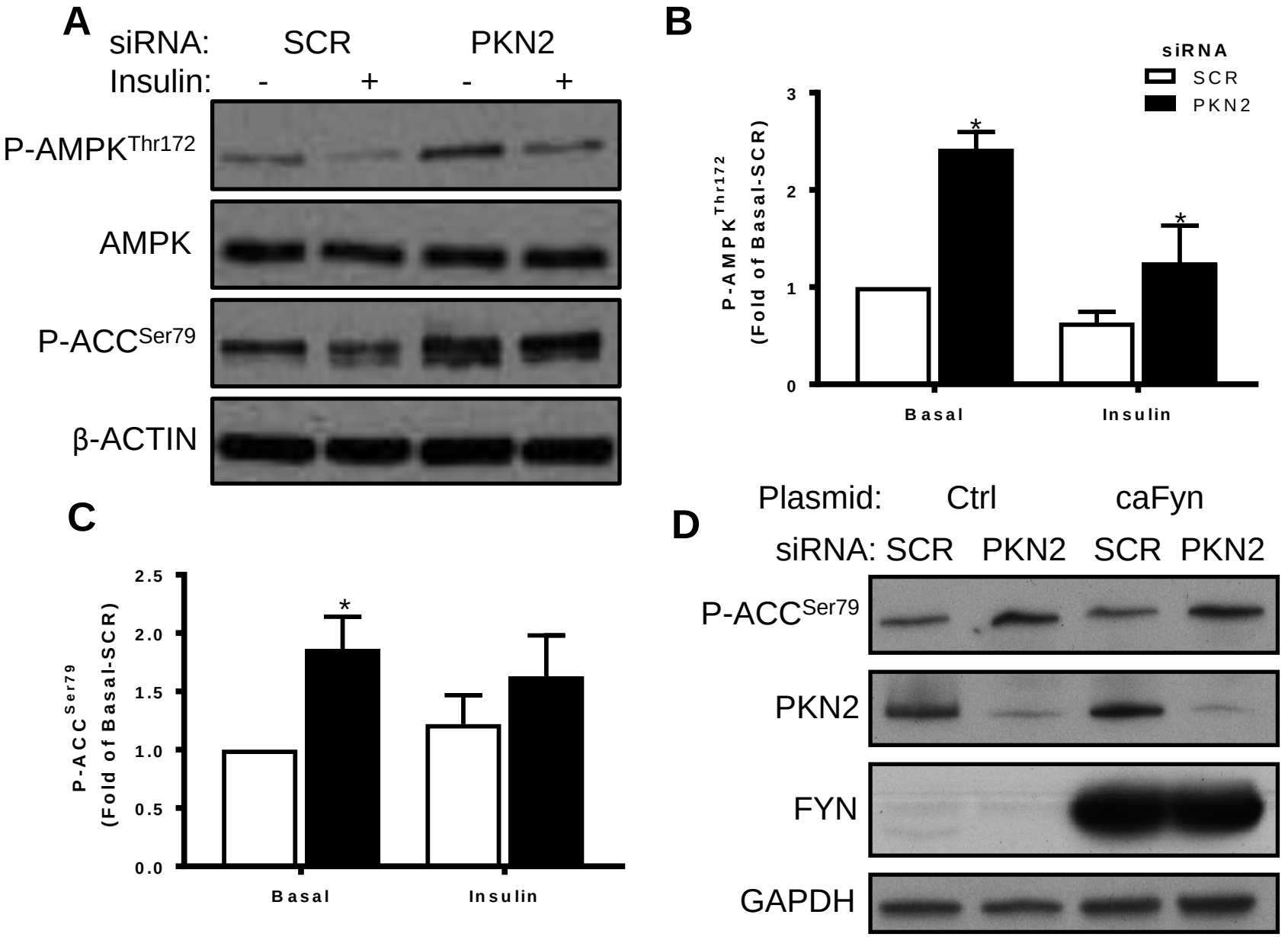
A
siRNA: SCR PKN2
Insulin: - + - +
P-AMPKThr172
AMPK
P-ACCSer79
β-ACTIN
B
siRNA
SCR
PKN2
P-AMPKThr172 (Fold of Basal-SCR)
3
2
1
0
*
*
Basal
Insulin
C
P-ACCSer79 (Fold of Basal-SCR)
2.5
2.0
1.5
1.0
0.5
0.0
*
Basal
Insulin
D
Plasmid: Ctrl caFyn
siRNA: SCR PKN2 SCR PKN2
P-ACCSer79
PKN2
FYN
GAPDH

Figure 4

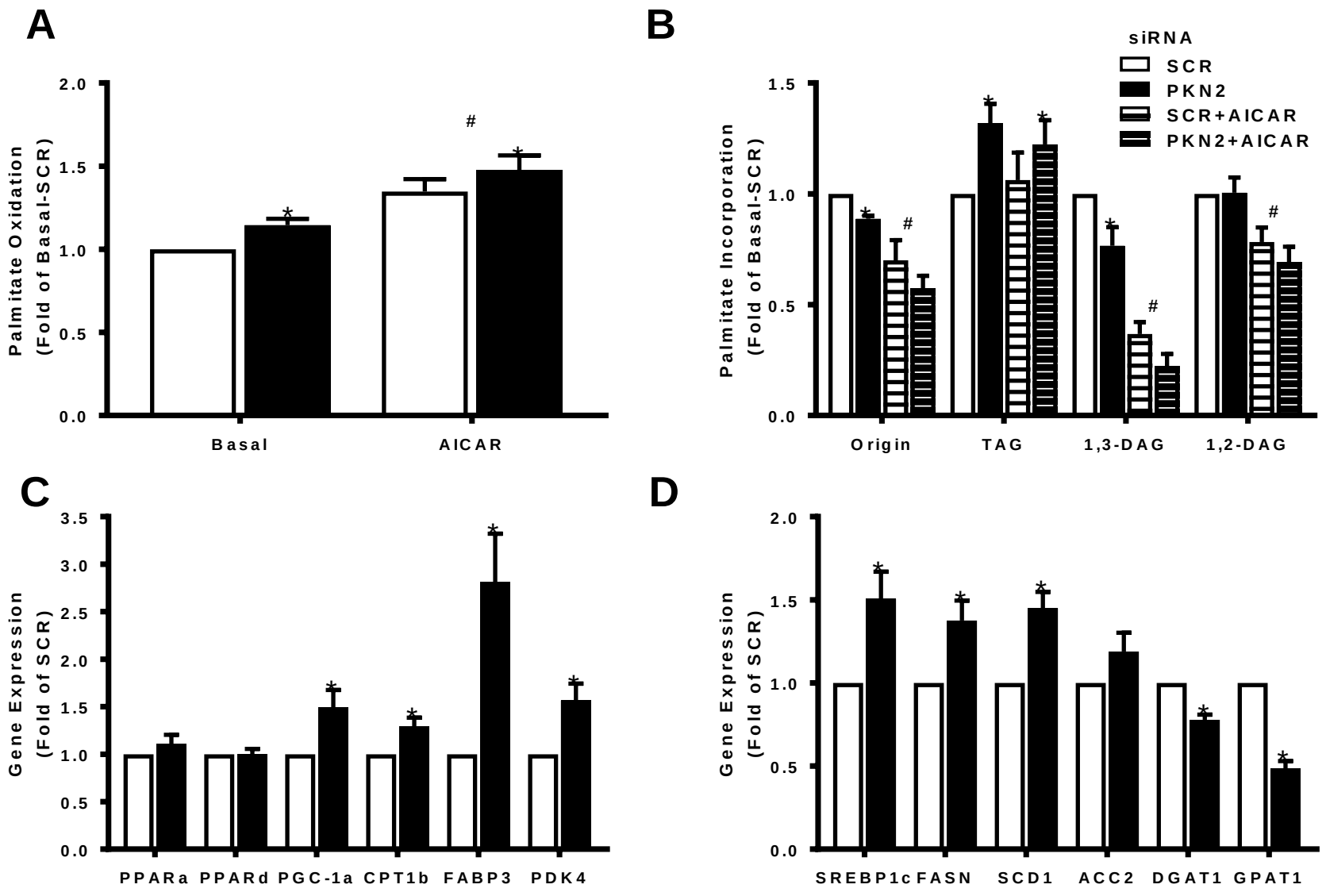
A
Palmitate Oxidation (Fold of Basal-SCR)
2.0
1.5
1.0
0.5
0.0
#
*
*
Basal
AICAR
B
siRNA
SCR
PKN2
SCR+AICAR
PKN2+AICAR
Palmitate Incorporation (Fold of Basal-SCR)
1.5
1.0
0.5
0.0
*
#
*
*
*
#
#
Origin
TAG
1,3-DAG
1,2-DAG
C
Gene Expression (Fold of SCR)
3.5
3.0
2.5
2.0
1.5
1.0
0.5
0.0
*
*
*
*
PPARa
PPARd
PGC-1a
CPT1b
FABP3
PDK4
D
Gene Expression (Fold of SCR)
2.0
1.5
1.0
0.5
0.0
*
*
*
*
*
SREBP1c
FASN
SCD1
ACC2
DGAT1
GPAT1

Figure 5

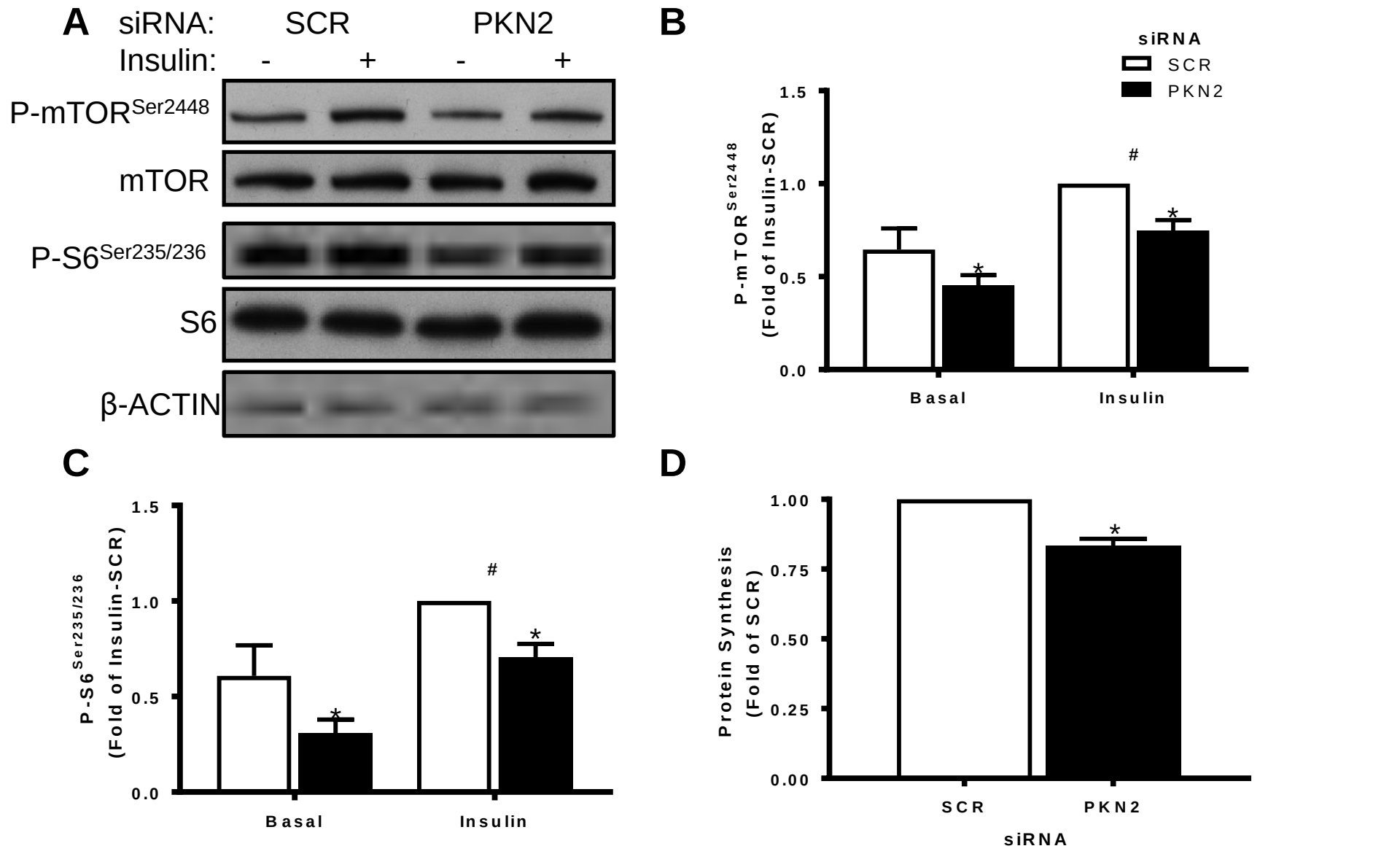
A
siRNA:
SCR
PKN2
Insulin:
-
+
-
+
P-mTOR Ser2448
mTOR
P-S6 Ser235/236
S6
β-ACTIN
B
siRNA
SCR
PKN2
P-mTOR Ser2448 (Fold of Insulin-SCR)
1.5
1.0
0.5
0.0
#
*
*
Basal
Insulin
C
P-S6 Ser235/236 (Fold of Insulin-SCR)
1.5
1.0
0.5
0.0
#
*
*
Basal
Insulin
D
Protein Synthesis (Fold of SCR)
1.00
0.75
0.50
0.25
0.00
*
SCR
PKN2
siRNA

Figure 6

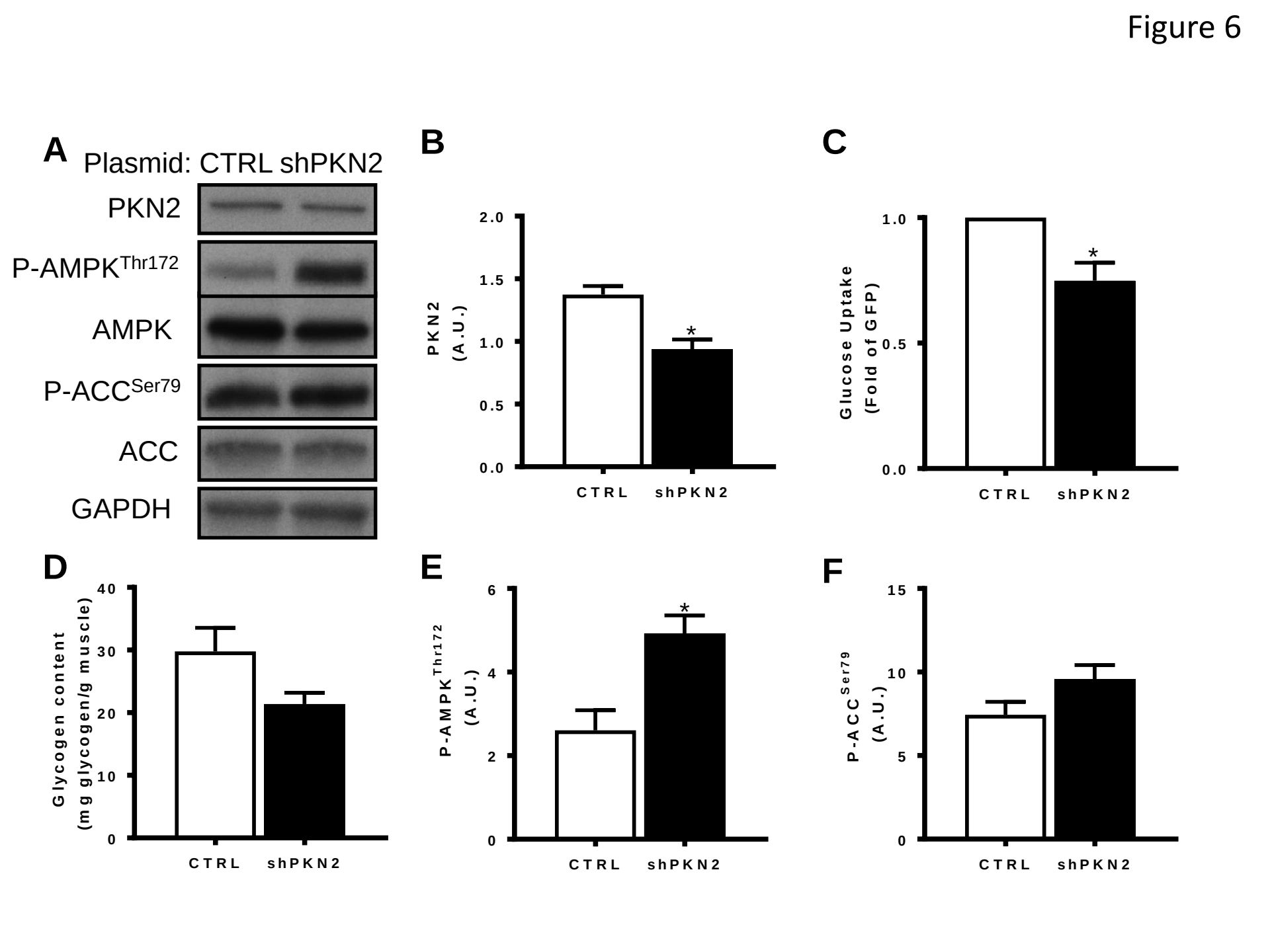
A
Plasmid: CTRL shPKN2
PKN2
P-AMPK Thr172
AMPK
P-ACC Ser79
ACC
GAPDH
B
PKN2 (A.U.)
2.0
1.5
1.0
0.5
0.0
*
CTRL
shPKN2
C
Glucose Uptake (Fold of GFP)
1.0
0.5
0.0
*
CTRL
shPKN2
D
Glycogen content (mg glycogen/g muscle)
40
30
20
10
0
CTRL
shPKN2
E
P-AMPK Thr172 (A.U.)
6
4
2
0
*
CTRL
shPKN2
F
P-ACC Ser79 (A.U.)
15
10
5
0
CTRL
shPKN2